

Stability of three-dimensional metallic glass

$\text{Ni}_{68}\text{B}_{21}\text{Si}_{11}$

DELIN LI, GENCANG YANG, YAOHE ZHOU

Laboratory 403, NW Polytechnical University, Xi'an 710072, People's Republic of China

BAOGEN SHEN

Institute of Physics, Academia Sinica, Beijing 100080, People's Republic of China

Under isothermal and linear heating conditions, the thermal stability of the three-dimensional metallic glass $\text{Ni}_{68}\text{B}_{21}\text{Si}_{11}$, produced by rapid quenching of the denucleated melt (RQDM), has been systematically studied using PE DSC7 differential scanning calorimetry in relation to denucleation of liquid alloy prior to rapid quenching, pre-anneal treatment of amorphous specimens, and cooling rate. The following results were observed. First, the thermal stability of metallic glass prepared by RQDM is obviously enhanced because of the removal of pre-existing nuclei in advance. This is substantiated by the experimental data showing that the projected life of three-dimensional metallic glass $\text{Ni}_{68}\text{B}_{21}\text{Si}_{11}$ is increased by an order of magnitude at 400 K. Secondly, pre-anneal treatment of the amorphous alloy leads to a reduction of temperature for the onset of crystallization, T_x , and crystallization heat, ΔH . Finally, quenching rates have little effect on the thermal stability of amorphous alloys.

1. Introduction

Amorphous alloys have many excellent physical, chemical and mechanical properties, but the size limitation and thermal instability of the alloys prevent their widespread application. In recent years, the technique of rapid quenching of the denucleated melt (RQDM) has been proposed to produce three-dimensional amorphous alloys [1]. Therefore, the properties, especially the thermal stability, of the three-dimensional metallic glasses are followed with great interest. Amorphous metal is not in an internal equilibrium state and will crystallize to stable phases under certain environments. In addition to determining the application limit conditions, a study of the crystallization process is of scientific significance, by offering a unique opportunity to reveal crystal growth at large undercooling. Of particular importance in all aspects of crystallization is the improvement of the thermal stability of metallic glasses. In the present work, further studies on the thermal stability of three-dimensional metallic glass $\text{Ni}_{68}\text{B}_{21}\text{Si}_{11}$ produced by RQDM, and its influencing factors, including liquid denucleation prior to rapid quenching, pre-anneal treatment of amorphous specimens and quenching rate, have been carried out.

2. Experimental procedure and kinetic equations

Amorphous samples of $\text{Ni}_{68}\text{B}_{21}\text{Si}_{11}$ of three-dimensional size have been successfully prepared by the RQDM method in which the basic experimental

procedure is as follows: high undercooling attainment by fluxing B_2O_3 and successive heating-cooling cycles, with subsequent rapid quenching of the denucleated melts. Thermal analysis and pre-anneal treatment were performed using PE DSC7 differential scanning calorimetry. The measurements of temperature and energy were calibrated using high-purity indium and zinc. Crystallization kinetics of amorphous alloys have been studied in the light of the classical theory of the Johnson-Mehl-Avrami (JMA) equation, especially for the isothermal crystallization process [2]

$$x = 1 - \exp(-kt^n) \quad (1)$$

where x is the crystallized volume fraction at time t minus the incubation time of crystallization, k is a kinetic parameter related to the temperature, nucleation rate and growth rate, n is the Avrami exponent which reflects the characteristics of nucleation and growth process during the transformation. The dependence of k on temperature, T , is expressed as

$$k = k_0 \exp(-E/RT) \quad (2)$$

Hence the transformation rate equation can be written

$$\frac{dx}{dt} = nk^{\frac{1}{n}}(1-x)[-\ln(1-x)]^{(n-1)/n} \quad (3)$$

where E is the activation energy of crystallization, k_0 a constant, and R the gas constant. The JMA equation can also be applied to the non-isothermal case if the crystallization mechanisms belong to isokinetics, which means that the crystallized fraction is independent of

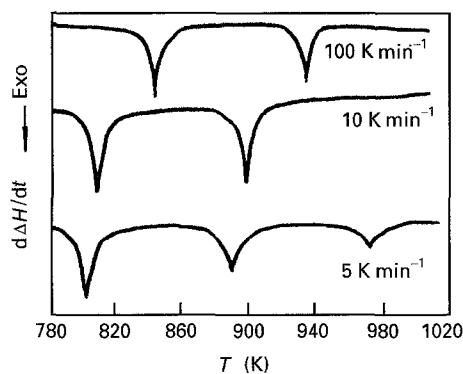


Figure 1 DSC curves of the as-quenched glass $\text{Ni}_{68}\text{B}_{21}\text{Si}_{11}$.

the thermal history. In fact, most of amorphous alloys including glass $\text{Ni}_{68}\text{B}_{21}\text{Si}_{11}$ meet the requirements. Integration of Equation 3 assuming a linear heating rate, β , a constant activation energy, E , and $E/RT \gg 2$, can yield the Kissinger equation

$$\ln \frac{T_w^2}{\beta} = \frac{E}{RT_w} + \text{constant} \quad (4)$$

T_w is the temperature when a specific crystallized fraction, x , is formed at heating rate, β . From multiple-scan DSC experiments, E , equal to the slope fitting the curve $\ln T_w^2/\beta$ versus $1/T_w$, can be calculated.

3. Results and discussion

DSC plots of the glass $\text{Ni}_{68}\text{B}_{21}\text{Si}_{11}$ exhibit two distinct exothermic peaks at the heating rate, $\beta \geq 10 \text{ K min}^{-1}$, while the third peak appears at about 970 K when β is below 10 K min^{-1} , as shown in Fig. 1. Further stabilization and ordering of some crystallization phases within an amorphous matrix bring about the third exothermic peak under slow heating conditions. When the heating rate is fast, the so-called stabilization process is considered to be suppressed. From a viewpoint of application limits, the parameters of the first crystallization peak are used to represent the thermal stability of amorphous alloys because "ductile-brittle" transformation often occurs when the amorphous specimens undergo the first peak.

3.1. Effects of liquid denucleation

Table I shows the crystallization parameters of three batches of glass $\text{Ni}_{68}\text{B}_{21}\text{Si}_{11}$ which were treated

differently prior to rapid quenching. The specimens of group A were produced by directly rapidly quenching the parent melt. The liquid alloy used to prepare the specimens of group B was undercooled by a range of 200–300 K, while a high undercooling up to 450 K was attained for group C.

As can be readily seen from Table I, T_x of group C is 6.3 K higher than that of group A at a heating rate $\beta = 5 \text{ K min}^{-1}$, but this difference is lessened to 1.6 K when β increases to 100 K min^{-1} . The peak temperature, T_p , of groups A and C changes with a similar trend to T_x . T_x and T_p of group B lie between those of groups A and C. It is worth pointing out that the mean crystallization heat has approximately the same values, which are $\Delta H_A = 72.2 \text{ J g}^{-1}$, $\Delta H_B = 70.8 \text{ J g}^{-1}$, and $\Delta H_C = 72.7 \text{ J g}^{-1}$, respectively. This implies that the three batches of $\text{Ni}_{68}\text{B}_{21}\text{Si}_{11}$ specimens are fairly comparable in their amorphousness, otherwise the results of the thermal analysis are not convincing. Although T_x can be taken as one of the important parameters for assessment of the thermal stability, the activation energy essentially reflects the nucleation barrier (potential well) from non-crystalline to crystalline structure. The larger is E , the more stable is the glass and the longer is the time for the start of crystallization, τ . For glass Ni–B–Si, τ can be described by an Arrhenius-type equation for a thermally activated process

$$\tau = \tau_0 \exp(E/RT) \quad (5)$$

where τ_0 is a constant. E for the above three batches of amorphous specimens can be calculated from a basically straight line of $\ln(T_x^2 \beta^{-1})$ against T_x^{-1} using the Kissinger method, as $E_A = 344 \text{ K J mol}^{-1}$, $E_B = 349 \text{ K J mol}^{-1}$, and $E_C = 352 \text{ K J mol}^{-1}$, as illustrated in Fig. 2. For instance, if the metallic glass works at 400 K, the ratio of the times for the beginning of crystallization can be calculated: $\tau_A : \tau_B : \tau_C = 1.0 : 4.5 : 11.0$. We concluded, therefore, that the projected life at 400 K of glass $\text{Ni}_{68}\text{B}_{21}\text{Si}_{11}$ produced by RQDM is enhanced by one order of magnitude. This is primarily because of the elimination of heterogeneous nucleation centres in advance.

With the aid of glass formation kinetics during rapid quenching, CCT curves constructed by Davies and Lewis [3] can be schematically plotted to analyse the effects of pre-existing nuclei within the amorphous alloy and heating rate, β , upon the crystallization. Supposing the pre-existing nuclei density, $N_1 > N_2 > N_3$ corresponding to three batches A, B and

TABLE I Onset temperature, T_x , peak temperature, T_p , and crystallization heat, ΔH , of $\text{Ni}_{68}\text{B}_{21}\text{Si}_{11}$ glass produced from differently denucleated melts

β (K min^{-1})	T_x (K)			T_p (K)			ΔH (J g^{-1})		
	A	B	C	A	B	C	A	B	C
5	786.1	790.0	792.4	796.6	798.4	799.5	77.4	66.8	74.0
10	798.8	802.1	803.6	806.6	807.6	807.9	71.5	71.0	69.9
20	808.5	810.2	811.4	816.1	816.5	817.0	68.4	67.2	74.2
50	824.0	825.5	826.0	831.5	831.6	831.4	74.6	73.5	73.7
100	834.7	835.9	836.3	844.6	844.8	844.7	69.0	75.6	71.8

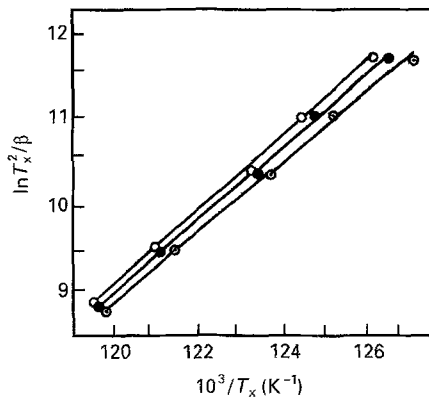


Figure 2 Kissinger plots of $\text{Ni}_{68}\text{B}_{21}\text{Si}_{11}$ glass produced from variously denucleated melts. A, master melt; B, undercooling $\Delta T = 200\text{--}300\text{ K}$; C, $\Delta T = 400\text{--}450\text{ K}$. (\odot) $E_A = 344\text{ kJ mol}^{-1}$, (\bullet) $E_B = 349\text{ kJ mol}^{-1}$, (\circ) $E_C = 352\text{ kJ mol}^{-1}$.

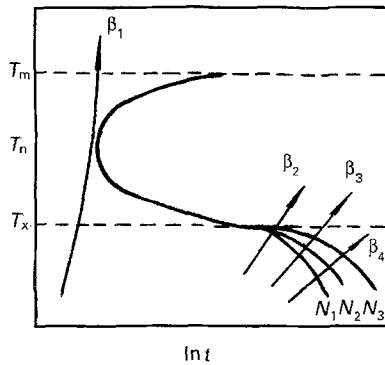


Figure 3 CCT curves of glass crystallization. N = number of nuclei ($N_1 > N_2 > N_3$); β = heating rate ($\beta_1 > \beta_2 > \beta_3 > \beta_4$).

C in Table I, respectively, and heating rate $\beta_1 > \beta_2 > \beta_3 > \beta_4$, the variation of T_x is clearly depicted in Fig. 3. When slowly heated at β_4 , the crystal nucleation mechanism of glass is dominated by the pre-existing nuclei, thus leading to an obvious difference among the T_x of the respective curves N_1 , N_2 and N_3 . However, this difference can be hardly observed as achieving a higher heating rate of β_2 , because the bulk homogeneous nucleation may prevail over the heterogeneous nucleation. The experimental results basically support the surface and bulk crystallization of Ni-7Si-17B amorphous alloy occurring, respectively, at low and high annealing temperature [4]. If it were possible to heat sufficiently quickly to pass the nose of the diagram, crystallization could be totally avoided. The relationship between the crystallization temperature and nuclei density and heating rate ascertained through the experiments and theoretical analysis, is in reasonable agreement, i.e. denucleation of melts has a notable impact on crystallization temperature under slow heating conditions, while little influence exists at the higher heating rate.

3.2. Effects of pre-anneal treatment

In order to study further the effects of pre-existing nuclei on the thermal stability, a procedure of pre-anneal treatment was designed as follows. The

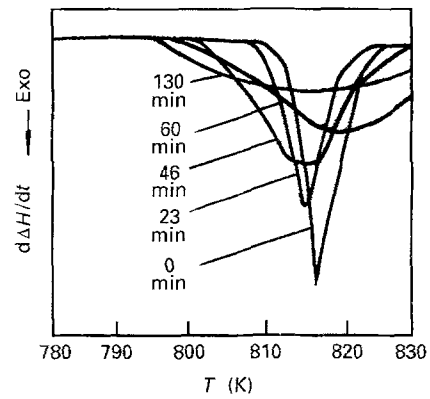


Figure 4 DSC curves of $\text{Ni}_{68}\text{B}_{21}\text{Si}_{11}$ glass pre-annealed at 753 K for different times (min).

as-quenched $\text{Ni}_{68}\text{B}_{21}\text{Si}_{11}$ glassy specimens produced by RQDM were heated at 753 K (about 50 K below the T_x) and held for 23, 46, 60, and 130 min, respectively, before quickly cooling to ambient temperature. Subsequently, the crystallization behaviour of the as-quenched samples and the pre-annealed samples was examined using the DSC7 at $\beta = 20\text{ K min}^{-1}$, as illustrated in Fig. 4. Three points should be addressed here. First crystallization temperature, T_x , and heat, ΔH , considerably decrease with an increase of pre-anneal time, which can be understood by the formation of new embryos, even microcrystalline clustering, during pre-anneal treatment. Secondly, the difference between T_p and T_x , ($T_p - T_x$), increases and the exothermal peaks become flattened with increasing pre-anneal time. The reduction of the maximum transformation rate represented by the peak height of the DSC curve probably arises from the handicap of atom diffusion in the presence of many nuclei after a long-term pre-anneal. Thirdly, T_p is slightly lowered after the amorphous samples are pre-annealed for 23 and 46 min, respectively, while for 60 and 130 min, T_p increases. The experimental results disagree with those of Lu and Wang [5].

3.3. Effects of quenching rate

The quenching rate is an important kinetic factor for forming glass metals, but its effects on the thermal stability are ambiguous and often contradictory [6, 7]. In our work, the quenching rate was altered by adjusting the substrate temperature and the thickness of the quenched specimens. For example, the substrate temperature may vary from room temperature ($\sim 300\text{ K}$) to liquid-nitrogen temperature ($\sim 80\text{ K}$). A series of DSC data on the amorphous specimens prepared in liquid-nitrogen-cooled substrate, has indicated that T_x and ΔH almost remain unchangeable: $T_x = 803.6\text{ K}$, $\Delta H = 71.0\text{ J g}^{-1}$ at $\beta = 10\text{ K min}^{-1}$. It is suggested that the thermal properties are not affected by quenching rate, as long as it is higher than the critical cooling rate for freezing the melt into the so-called entire amorphous structure. When the room-temperature substrate is used, fluctuations of T_x and ΔH for quenched amorphous specimens can be found from Table II. This indicates that the quenching rate below the

TABLE II DSC analysis results of $\text{Ni}_{68}\text{B}_{21}\text{Si}_{11}$ glass prepared with room-temperature substrate

	1	2	3	4	5
T_x (K)	799.7	802.4	804.0	795.2	793.0
ΔH (J g^{-1})	69.0	71.8	71.8	43.7	29.6

critical cooling rate will result in an amorphous structure consisting of a quantity of nuclei, or even a mixed structure of amorphous and microcrystalline phase. In this case, the drop of T_x is always followed by a decrease in ΔH , a sign of amorphous deterioration. In fact, this should not be attributed to the effects of quenching rate on the thermal stability of metallic glass. It was reported that amorphous alloy $\text{Ni}_{75}\text{B}_{17}\text{Si}_8$ up to $225 \mu\text{m}$ thick was obtained [8], but the onset crystallization temperature, T_x , and heat ΔH decrease when the thickness of these samples is over $100 \mu\text{m}$. The results also provide evidence for the above analysis. By the way, it is well recognized that the glass transition temperature, T_g , is displaced to higher temperature when the quenching rate is increased, but T_g dose not change very much.

4. Conclusion

Not only can three-dimensional amorphous alloys be prepared by RQDM, but also this technique opens a new window for improving the thermal stability of amorphous alloys. At a heating rate of 5 K min^{-1} , the

onset crystallization temperature of a three-dimensional glass $\text{Ni}_{68}\text{B}_{21}\text{Si}_{11}$ is 6.3 K higher than that of glass samples which are not denucleated prior to rapid quenching. Moreover, the crystallization activation energy increases by 2.3%. Pre-anneal treatment of amorphous alloys causes a fall in the onset crystallization temperature and crystallization heat. The quenching rate has little influence on the thermal stability, unless it is below the critical cooling rate for glass formation.

References

1. D. L. LI, G. C. YANG and Y. H. ZHOU, *J. Mater. Sci. Lett.* **11** (1992) 1033.
2. A. CALKA and A. P. RADLINSKI, *Mater. Sci. Eng.* **97** (1988) 241.
3. H. A. DAVIES and B. G. LEWIS, in "Proceedings of Rapidly Quenched Metals II", Section I, Cambridge, November 1975, edited by N. J. Grant and B. C. Giessen (MIT, Cambridge, 1976) p. 259.
4. M. H. ZUERCHER and D. G. MORRIS, *J. Mater. Sci.* **23** (1988) 515.
5. K. LU and J. T. WANG, *Mater. Sci. Eng.* **97** (1988) 399.
6. A. L. GREER and A. J. DREHMAN, *Acta Metall.* **32** (1984) 323.
7. C. S. KIMINAMI and P. R. SAHM, *ibid.* **34** (1986) 2129.
8. M. HAGIWARA, A. INOUE and T. MASUMOTO, *Metall. Trans. A12* (1981) 1027.

Received 22 October 1993
and accepted 27 July 1994